Biochemical and Biophysical Research Communications 459 (2015) 387–392

Contents lists available at ScienceDirect

Biochemical and Biophysical Research Communications

journal homepage: www.elsevier.com/locate/ybbrc

Structural insights into domain movement and cofactor specificity of glutamate dehydrogenase from *Corynebacterium glutamicum*

Hyeoncheol Francis Son [a], Il-Kwon Kim [b], Kyung-Jin Kim [a, *]

[a] School of Life Sciences, KNU Creative BioResearch Group, Kyungpook National University, Daehak-ro 80, Buk-ku, Daegu 702-701, Republic of Korea
[b] Paik Kwang Industrial Company Ltd., 57 Oehang-4 Gil, Gunsan, Jellabuk-do 573-879, Republic of Korea

ARTICLE INFO

Article history:
Received 12 February 2015
Available online 27 February 2015

Keywords:
Glutamate dehydrogenase
Corynebacterium glutamicum
Cofactor specificity
Structure

ABSTRACT

Glutamate dehydrogenase (GDH) is an enzyme involved in the synthesis of amino acids by converting glutamate to α-ketoglutarate, and vice versa. To investigate the molecular mechanism of GDH, we determined a crystal structure of the *Corynebacterium glutamicum*-derived GDH (*Cg*GDH) in complex with its NADP cofactor and α-ketoglutarate substrate. *Cg*GDH functions as a hexamer, and each *Cg*GDH monomer comprises 2 separate domains; a Rossmann fold cofactor-binding domain and a substrate-binding domain. The structural comparison between the apo- and cofactor/substrate-binding forms revealed that the *Cg*GDH enzyme undergoes a domain movement during catalysis. In the apo-form, *Cg*GDH exists as an open state, and upon binding of the substrate and cofactor the protein undergoes a conformation change to a closed state. Our structural study also revealed that *Cg*GDH has cofactor specificity for NADP, but not NAD, and this was confirmed by GDH activity measurements. Residues involved in the stabilization of the NADP cofactor and the α-ketoglutarate substrate were identified, and their roles in substrate/cofactor binding were confirmed by site-directed mutagenesis experiments.

1. Introduction

Synthesis of amino acids is a vital process in almost all organisms, and nitrogen metabolism is a key reaction in this process. Glutamate dehydrogenases (GDHs) are involved in the tricarboxylic acid cycle and convert L-glutamate to α-ketoglutarate (2-oxoglutarate) through the oxidative deamination reaction. The reductive amination reaction using α-ketoglutarate provides nitrogen for several other biosynthetic pathways [1].

Based on their cofactor specificity, GDH enzymes can be categorized into 3 sub-families; NAD(H)-dependent (EC 1.4.1.2), NADP(H)-dependent (EC 1.4.1.4), and NAD(H)/NADP(H) dual-specific GDHs (EC 1.4.1.3) [2]. NAD(H)-dependent GDHs are commonly involved in glutamate catabolism, whereas NADP(H)-dependent GDHs are required for ammonium assimilation [3]. The dual-specific mammalian GDHs can utilize both NAD(H) and NADP(H) cofactors with comparable efficacy, and are known to be allosterically controlled by small molecules [3–5].

GDHs have been isolated and sequenced from various organisms and can be divided into 2 different types based on their oligomeric states. NADP(H)-specific bacterial and fungal GDHs and NAD(H)/NADP(H) dual-specific vertebrate GDHs function in hexameric form, with a molecular weight per subunit of approximately 50 kDa. NAD(H)-dependent GDHs have either a hexameric structure with around 48 kDa molecular weight, or have a tetrameric structure with around 115 kDa molecular weight [4,6–8]. Generally, in hexameric GDHs from bacteria, each subunit divides into 2 domains, with a deep cleft between each domain. The N-terminal substrate-binding domain is involved in hexamer formation and the C-terminal cofactor (NAD(H)/NADP(H)) binding domain exhibits a modified Rossmann fold [6].

In the present study, we report a crystal structure of GDH from *Corynebacterium glutamicum* (*Cg*GDH) in an apo-form and in complex with its cofactor and substrate. Based on the structural and biochemical studies of *Cg*GDH, we also reveal that the enzyme undergoes an open/closed conformational change upon binding of its cofactor and substrate. Using site-directed mutagenesis experiments, we also identified residues involved in the stabilization of the NADP cofactor and α-ketoglutarate substrate.

* Corresponding author. Structural and Molecular Biology Laboratory, School of Life Sciences, Kyungpook National University, Daehak-ro 80, Buk-ku, Daegu 702-701, Republic of Korea. Fax: +82 53 955 5522.
E-mail address: kkim@knu.ac.kr (K.-J. Kim).

http://dx.doi.org/10.1016/j.bbrc.2015.02.109
0006-291X/

2. Materials & methods

2.1. Cloning, expression and purification

Cloning, expression, purification, and crystallization of *Cg*GDH will be described in detail elsewhere (Son et al., in preparation). Briefly, the *Cg*GDH coding gene was amplified by polymerase chain reaction (PCR) using genomic DNA from *C. glutamicum* strain ATCC 13032 as a template. The PCR product was then subcloned into pProEX-HTa (Invitrogen) resulting in a 6x-histag followed by a TEV protease (rTEV) cleavage site at the N-terminus. The resulting expression vector pProEX-HTa:*Cg*GDH was transformed into an *Escherichia coli* BL21(DE3)-T1^{R} strain, which was grown in 1 L of LB medium containing 100 mM ampicillin at 37 °C. At an OD_{600} of 0.6, expression of *Cg*GDH protein was induced by adding 1 mM IPTG, and the culture medium was maintained for a further 20 h at 18 °C. The culture was harvested by centrifugation at 4000 × *g* for 20 min at 4 °C. The resulting cell pellet was resuspended in buffer A (40 mM Tris–HCl, pH 8.0) and disrupted by ultrasonication. The cell debris was removed by centrifugation at 13,500 g for 25 min and the lysate was applied to an Ni-NTA agarose column (Qiagen). After washing with buffer A containing 30 mM imidazole, the bound proteins were eluted with 300 mM imidazole in buffer A. The 6x-histag was removed by treatment with rTEV. Finally, trace amounts of contaminants were removed by size-exclusion chromatography using a Superdex 200 prep-grade column (320 ml, GE Healthcare) equilibrated with buffer A. All purification experiments were performed at 4 °C.

2.2. Crystallization, data collection, and structure determination

Crystallization of the purified *Cg*GDH protein was initially performed with commercially available sparse-matrix screens, including Index, PEG ion I and II (Hampton Research), Wizard Classic I and II, Wizard CRYO I and II (Rigaku) and Structure Screen I and II (Molecular Dimensions), all using the sitting-drop vapor-diffusion method at 20 °C. Each experiment consisted of mixing 1.0 μl protein solution (140 mg/ml in 40 mM Tris–HCl, pH 8.0) with 1.0 μl reservoir solution and then equilibrating against 50 μl reservoir solution. The *Cg*GDH crystals of the best quality appeared in 17% polyethylene glycol 3350, 7% Tacsimate, pH 5.0 and 10 mM spermidine. The crystals were finished out with a loop larger than the crystals and flash-frozen by immersion in liquid nitrogen. Data were collected to a resolution of 2.3 Å at 7A beamline of the Pohang Accelerator Laboratory (PAL, Pohang, Korea), using a Quantum 270 CCD detector (ADSC, USA). All data were indexed, integrated, and scaled together using the HKL2000 software package [9]. The crystals of *Cg*GDH belonged to the space group $P2_1$. Assuming 12 *Cg*GDH molecules in an asymmetric unit, the crystal volume per unit of protein mass was 2.42 $Å^3$ Da^{-1}, which means the solvent content was approximately 49.16% [10].

The structure was determined by molecular replacement with the CCP4 version of MOLREP [11] using the structure of GDH from *Clostridium symbiosum* (PDB code 1BGV) as a search model. Model building was performed manually using the program WinCoot [12], and refinement was performed with CCP4 refmac5 [13] and CNS [14]. The data statistics are summarized in Table 1. The refined *Cg*GDH model will be deposited in the protein data bank.

2.3. Site-directed mutagenesis and activity assay

Site-specific mutations were created with the Quick Change kit (Stratagene), and sequencing was performed to confirm correct incorporation of the mutations. Mutant proteins were purified in the same manner as for wild type. For GDH activity assay, oxidation of NADPH to NADP was measured by monitoring the decrease of absorbance at 340 nm (extinction coefficient of 6.22×10^3 M^{-1} cm^{-1}). All assays were performed with reaction mixture of 1 ml total volume, and performed at 30 °C. The reaction mixture contained 100 mM Tris–HCl, pH 8.0, 250 μM NADPH or NADH, 20 mM ammonium chloride, and 10 mM α-ketoglutarate. The reaction was initiated by the addition of enzyme to a final concentration of 40.8 nM.

Table 1
Data collection and refinement statistics.

	*Cg*GDH
Data collection	
Space group	$P2_1$
Cell dimensions	
a, *b*, *c* (Å)	171.22, 93.032, 187.88
α, β, γ (°)	90.00, 108.16, 90.00
Resolution (Å)	50.00–2.30 (2.34–2.30)*
R_{sym} or R_{merge}	11.4 (29.9)
$I/\sigma(I)$	21.14 (5.36)
Completeness (%)	98.6 (95.8)
Redundancy	5.6 (4.2)
Refinement	
Resolution (Å)	178.51–2.30
No. reflections	1,364,094
R_{work}/R_{free}	16.8/22.6
No. atoms	42,473
Protein	40,318
Ligand/ion	522
Water	1633
B-factors	25.184
Protein	24.161
Ligand/ion	26.157
Water	26.466
R.m.s. deviations	
Bond lengths (Å)	0.0151
Bond angles (°)	1.8203

*Number of xtals for each structure should be noted in footnote. *Values in parentheses are for highest-resolution shell.
[AU: Equations defining various *R*-values are standard and hence are no longer defined in the footnotes.].
[AU: Ramachandran statistics should be in Methods section at the end of Refinement subsection.].
[AU: Wavelength of data collection, temperature and beamline should all be in Methods section.].

3. Results and discussion

3.1. Overall structure of CgGDH

In order to elucidate the cofactor specificity, oligomeric status, and reaction mechanism of glutamate dehydrogenase from *C. glutamicum* (*Cg*GDH), we determined a crystal structure of the protein at 2.3 Å. The asymmetric unit of the crystal contained 12 molecules, corresponding to 2 hexameric structures of the protein. The atomic structure was in good agreement with the X-ray crystallographic statistics for bond angles, bond lengths, and other geometric parameters (Table 1). The *Cg*GDH monomer consists of 2 core domains: a substrate-binding domain (Met1-Leu205, Gly368-Ser393 and Tyr425-Ile447) and a cofactor-binding domain (Val206-Pro367 and Phe394-Asp424) (Fig. 1). The substrate-binding domain consists of 10 α-helices (α1-α8, α15 and α17) and 4 β-strands (β1-β4). The 4 β-strands form a β-sheet packed in the middle of the substrate-binding domain and the 10 α-helices are located on both sides of the β-sheet. The cofactor-binding domain consists of 7 α-helices (α9-α14 and α-16) and 6 β-strands (β5-β10) and forms an NAD(H) and/or NADP(H)-binding Rossmann fold conformation. A classical Rossmann fold has a $\beta_1\alpha_1\beta_2\alpha_2\beta_3$-motif, with a second nucleotide-binding motif ($\beta_4\alpha_4\beta_5\alpha_5\beta_6$). The 2 motifs form a parallel

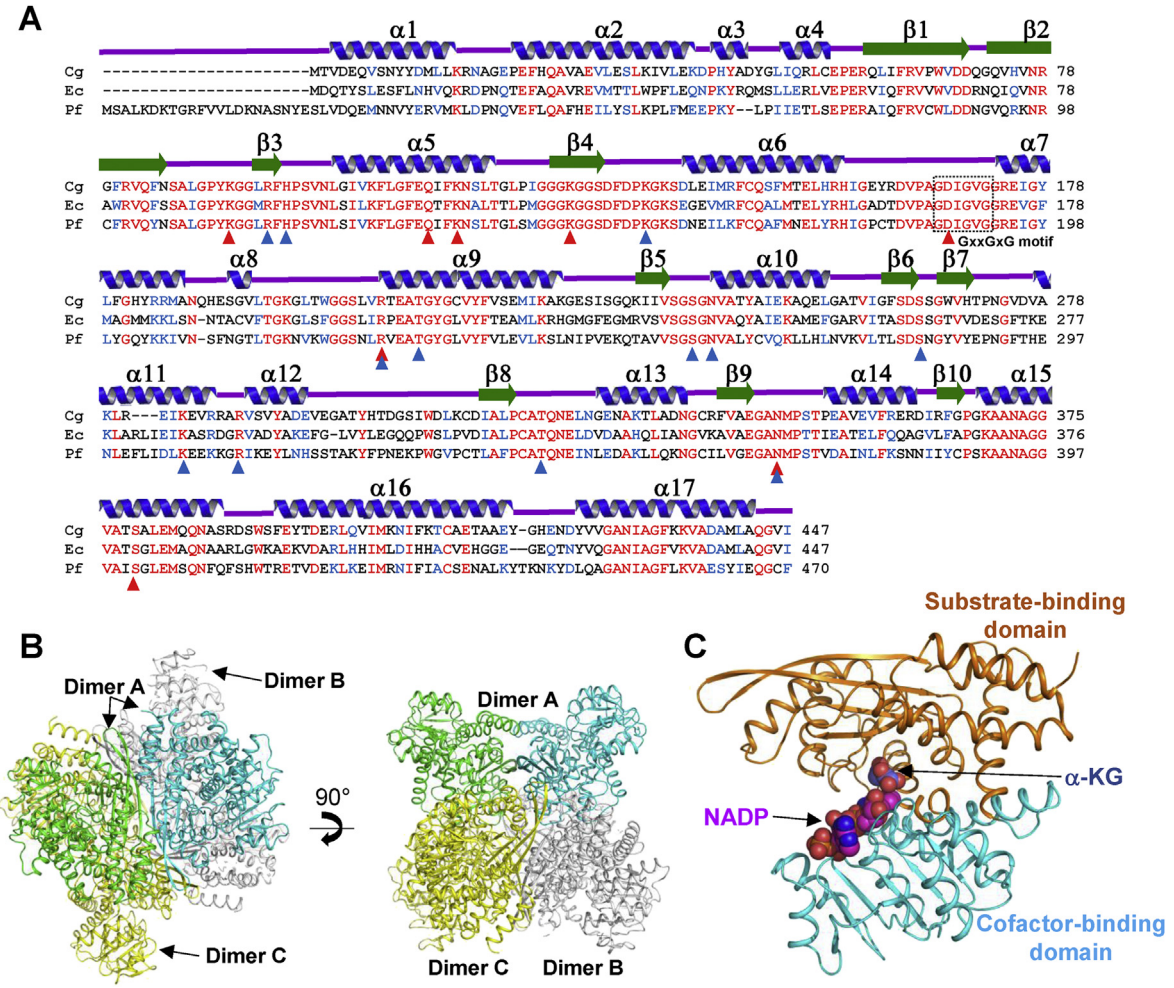

Fig. 1. Overall shape of *Cg*GDH. (A) Amino acid sequence alignment of glutamate dehydrogenases. Secondary structure elements are shown based on the *Cg*GDH structure. Identical and highly conserved residues are presented in red and blue colored characters, respectively. Residues involved in binding of NADP cofactor and α-ketoglutarate substrate are marked with blue and red colors, respectively. The GxxGxG motif is marked with a black-colored dotted rectangle, and labeled. Cg, Ec and Pf are abbreviations of *Corynebacterium glutamicum*, *Escherichia coli* and *Pyrococcus furiosus*, respectively. (B) Hexameric structure of *Cg*GDH. A *Cg*GDH hexamer was shown as a cartoon model. One *Cg*GDH dimer was distinguished with different colors of cyan and green, and other 2 dimers were with gray and yellow colors. The right side figure is 180° rotated horizontally from the left side figure. (C) Monomeric structure of *Cg*GDH. Monomeric structure of *Cg*GDH was shown as a cartoon diagram, and the substrate-binding domain and the cofactor-binding domain were distinguished with orange and cyan colors, respectively. The bound NADP and α-ketoglutarate were shown as sphere models with magentas and light-blue colors, respectively. (For interpretation of the references to color in this figure legend, the reader is referred to the web version of this article.)

β-sheet consisting of 6 β-strands and the β-sheet is surrounded by α-helices [15,16]. In *Cg*GDH, 2 βαβαβ-motifs exhibit a somewhat different arrangement of the order of their secondary structure elements. The first and the second motifs are ordered $\beta_5\alpha_{10}\beta_6\beta_7\alpha_{11}$ and $\beta_8\alpha_{13}\beta_9\alpha_{14}\beta_{10}$, respectively (Fig. 1). Like many other GDHs, *Cg*GDH forms a hexameric structure that corresponds to 3 dimers (Fig 1B). Dimerization is mediated by the contact between 2 substrate-binding domains: a parallel β-sheet (β1-β4) of one molecule contacts with that of the neighboring molecule forming an extended β-sheet. Three α-helices near the β-sheet also contribute to the dimerization. The formation of hexameric structure is also mediated by the substrate-binding domain.

3.2. Open/closed conformational change of *Cg*GDH

In our current *Cg*GDH structure, 2 different conformations are observed. Among the 12 molecules in the asymmetric unit, 3 molecules are in an apo-form, and 9 molecules are in complex with both the NADP cofactor and α-ketoglutarate substrate. When we superposed the cofactor-binding domains of the apo- and complex forms of *Cg*GDH, we observed that the relative positions of the substrate-binding domains were quite different from each other. In the substrate/cofactor-complex form, the substrate-binding domain intimately contacts the cofactor-binding domain, and a deep and narrow cleft is formed between these 2 domains where the substrate and the cofactor are tightly bound. However, in the apo-form, the substrate-binding domain is positioned apart from the cofactor-binding domain, and the substrate/cofactor-binding sites are wide open (Fig. 2A). Conformational change within the substrate-binding domain was not observed, but rather the domain itself moves a distance of ~15 Å (Fig. 2A). The α16 helix plays a role as an axis in the domain movement, and the hinge region is composed of 2 connecting loops (α15-α16 and α16-α17). Based on these observations, we propose that *Cg*GDH undergoes an open/closed conformational change during catalysis. Without substrate and cofactor binding, the protein exists as an open state, and upon binding of the substrate and cofactor, the protein undergoes a conformation change to a closed state (Fig. 2B).

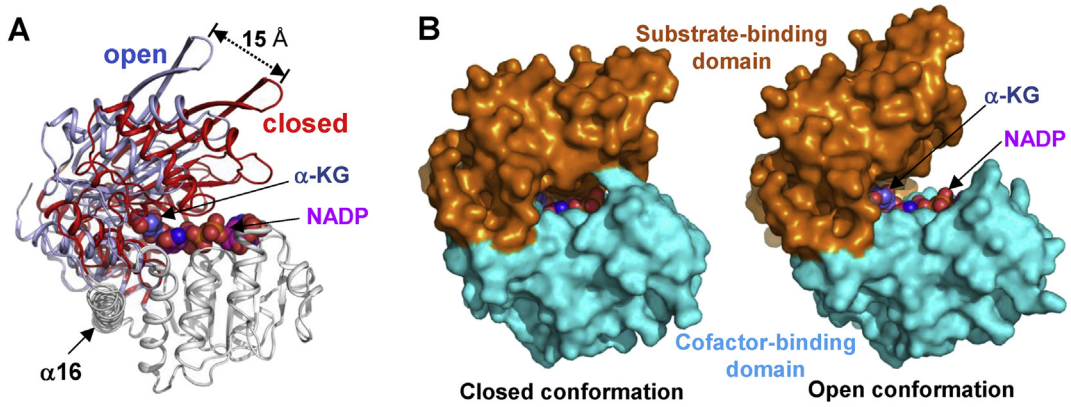

Fig. 2. Domain conformational change of *Cg*GDH. (A) Structural comparison of the open and closed conformations of *Cg*GDH. The cofactor-binding domains of the open and closed conformation of *Cg*GDH were superposed, and the relative positions of the substrate-binding domains were compared. The cofactor-binding domains of *Cg*GDH were shown with gray color, and the substrate-binding domains of the open and closed conformations of *Cg*GDH were with light-blue and red colors, respectively. The bound NADP and α-ketoglutarate were shown as sphere models with magentas and light-blue colors, respectively, and labeled. (B) Substrate binding mode of *Cg*GDH. The open and closed conformations of *Cg*GDH were shown as surface model. The substrate-binding domain and the cofactor-binding domain were distinguished with orange and cyan colors, respectively. The bound NADP and α-ketoglutarate were shown as sphere models with magentas and light-blue colors, respectively, and labeled. (For interpretation of the references to color in this figure legend, the reader is referred to the web version of this article.)

3.3. NADP binding mode of CgGDH

As described above, GDH enzymes can be categorized into 3 sub-families according to their cofactor specificity: NAD(H)-dependent, NADP(H)-dependent, and NAD(H)/NADP(H)-dependent enzymes. Because the NADP cofactor was observed to be bound in our current structure without addition of NADP in the crystallization conditions, we speculate that *Cg*GDH might utilize NADP(H) as a cofactor. In order to confirm the cofactor specificity of the enzyme, we tested GDH activity using either NADPH or NADH as a cofactor. As expected, *Cg*GDH showed strong activity using NADPH as a cofactor, whereas no activity was observed using NADH as a cofactor (Fig. 3A). This result confirms that *Cg*GDH is an NADP(H)-dependent GDH enzyme.

The NADP-binding pocket is mainly formed by the cofactor-binding domain, with partial contribution by the substrate-binding domain. The NADP-binding pocket is made up of 6 loops (β3-α5, β4-α6, β5-α10, α11-α12, β8-α13, and β9-α14), 1 α-helix (α9) and 1 β-strand are also involved (Fig. 2B). The G-x-x-G-x-G nucleotide-binding motif, comprising G167-D168-I169-G170-V171-G172, is observed in the substrate-binding domain and contributes to the stabilization of the pyrophosphate moiety of NADP. The nicotinamide ring is recognized by Arg208, Thr212, and Asn243, and the 2 ribose rings are stabilized through hydrogen bonding mediated by the side chains of Arg96, Ser241, Lys284, Arg290, Asp322, and Asn347. The adenine moiety is positioned next to the side chains of His98 and Ser265. The phosphate moiety is stabilized by residues Lys136, Ser245, Ser265, Lys284, and Arg290 through a direct and water-mediated hydrogen bond network, and we suspect that these residues provide NADP cofactor specificity to *Cg*GDH (Figs. 1A and 3B). The involvement of these residues in the stabilization of the phosphate moiety of NADP was further confirmed by site-directed mutagenesis experiments (Fig. 3A). Interestingly, the residues Arg96, His98, Lys136, and Asp322 are provided by the substrate-binding domain, and we propose that the NADP cofactor is unable to be tightly bound in the open form of *Cg*GDH.

3.4. Substrate binding mode of CgGDH

The α-ketoglutarate substrate is positioned within the deep cleft between the substrate-binding domain and the cofactor-binding domain of *Cg*GDH, and located in vicinity of the nicotinamide ring of NADP (Fig. 3). The substrate-binding pocket

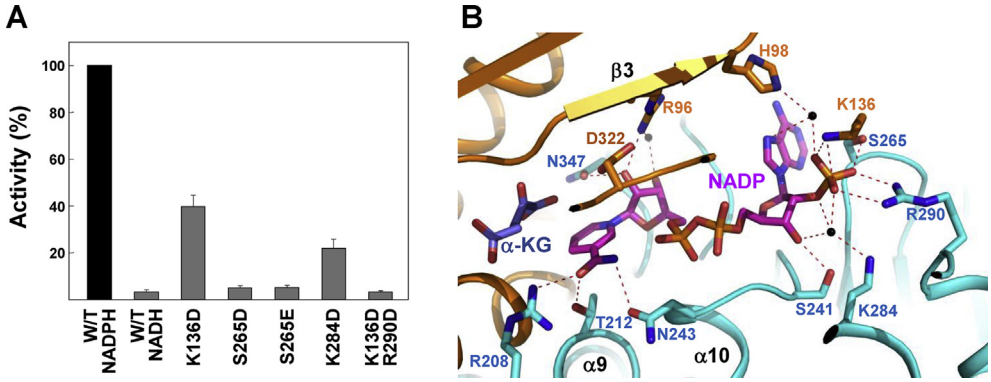

Fig. 3. Cofactor-binding mode of *Cg*GDH. (A) Cofactor specificity and site-directed mutagenesis. GDH activity of wild-type *Cg*GDH with NADPH was compared with that with NADH, Residues involved in the stabilization of the phosphate moiety of NADP cofactor were replaced by appropriate residues. The relative activities of recombinant mutant proteins were measured with NADPH as a cofactor and compared with that of wild-type *Cg*GDH. (B) Cofactor-binding mode of *Cg*GDH. The closed-form of *Cg*GDH was shown as cartoon diagram. The substrate-binding domain and the cofactor-binding domain were distinguished with orange and cyan colors, respectively. Regions involved in the NADP cofactor-binding were shown as stick model, and labeled appropriately. The bound NADP and α-ketoglutarate were shown as stick models with magentas and light-blue colors, respectively. Water molecules involved in the stabilization of NADP were shown as sphere model with black color. Red-colored dotted lines indicate hydrogen bonds contributing the binding of NADP. (For interpretation of the references to color in this figure legend, the reader is referred to the web version of this article.)

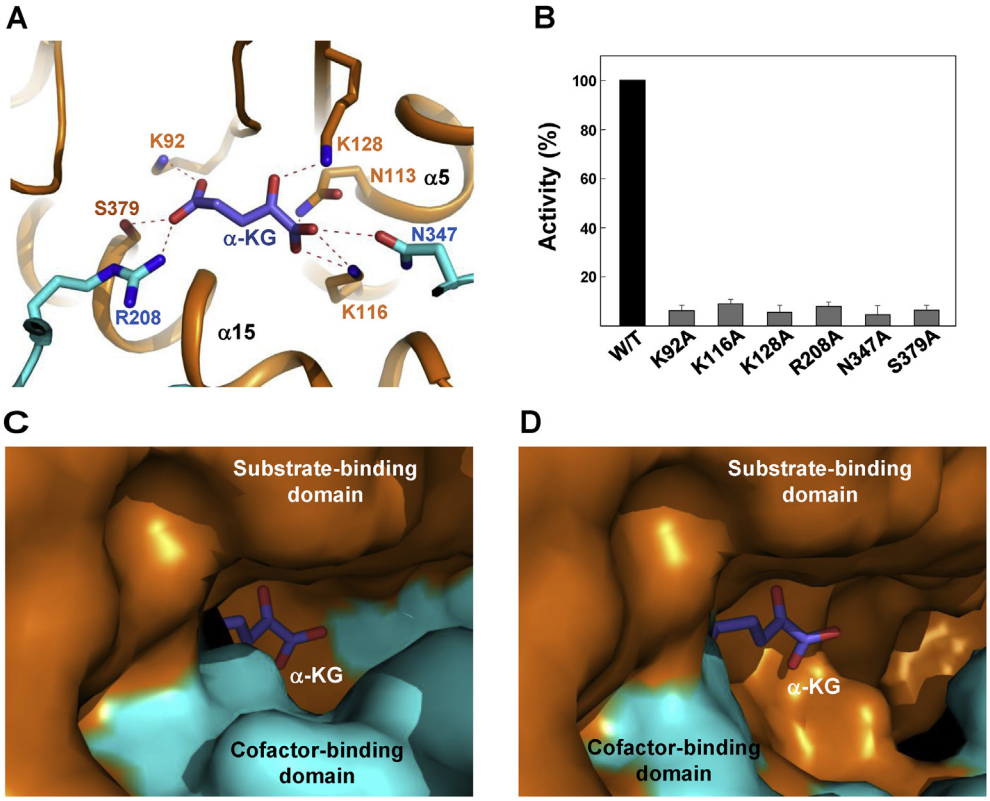

Fig. 4. Substrate-binding mode of *Cg*GDH. (A) Substrate-binding mode of *Cg*GDH. The closed form of *Cg*GDH was shown as cartoon diagram. The substrate-binding domain and the cofactor-binding domain were distinguished with orange and cyan colors, respectively. Regions involved in the substrate-binding were shown as stick model and labeled appropriately. The bound α-ketoglutarate and NADP were shown as stick model with magentas and light-blue colors, respectively. Red-colored dotted lines indicate hydrogen bonds contributing the binding of α-ketoglutarate. (B) Site-directed mutagenesis of *Cg*GDH. Residues involved in the substrate-binding were replaced by alanine residues. The relative activities of the recombinant mutant proteins were measured and compared with that of wild-type *Cg*GDH. (C) (D) Substrate-binding pockets of the closed (C) and open (D) forms of *Cg*GDH. The *Cg*GDH structures were shown as surface model. The substrate-binding domain and the cofactor-binding domain were distinguished with orange and cyan colors, respectively. The bound α-ketoglutarate was shown as stick model with light-blue color. (For interpretation of the references to color in this figure legend, the reader is referred to the web version of this article.)

consists of 4 loops (β2-β3, β4-α6, α8-α9, and β9-α14) and 2 α-helices (α5 and α15). The negatively charged α-ketoglutarate molecule is mostly stabilized by positively charged residues, such as Lys92, Lys116, Lys128, and Arg208, through charge–-charge interaction, although hydrogen bonds with Asn347 and Ser379 also contribute to substrate binding. In detail, the O1 and O2 atoms in one carboxyl-group form hydrogen bond with Lys116 and Asn347, and the O3 and O4 atoms in the other carboxyl-group form hydrogen bonds with Lys92, Arg208, and Ser379. Lys128 aids the stabilization of the carbonyl-group of the substrate through a hydrogen bond, and the residue might also be involved in the stabilization of the amide group of glutamate when this is used as a substrate. We also performed site-directed mutagenesis experiments by replacing the residues to alanine, and observed almost complete loss of activity from K92A, K116A, K128A, R208A, N347A, and S379A mutants. These results confirm the involvement of these residues in the stabilization of the α-ketoglutarate substrate. Moreover, as observed in the cofactor-binding of the enzyme, 2 residues (Arg208 and Asn347) are provided by the cofactor-binding domain, while other residues are located in the substrate-binding domain. Based on these observations, we propose that the *Cg*GDH enzyme adopts a closed conformation during catalysis (Fig. 4C,D).

Conflict of interest

None.

Acknowledgments

This work was supported by the National Research Foundation of Korea (NRF) Grant funded by the Korean Government (MEST) (2014R1A2A2A01005752 and NRF-2014M1A2A2033626) and by the Advanced Biomass R&D Center (ABC) of Global Frontier Project funded by the MEST (2012M3A6A2053895).

Transparency document

Transparency document related to this article can be found online at http://dx.doi.org/10.1016/j.bbrc.2015.02.109.

References

[1] K.L. Britton, P.J. Baker, P.C. Engel, D.W. Rice, T.J. Stillman, Evolution of substrate diversity in the superfamily of amino acid dehydrogenases. Prospects for rational chiral synthesis, J. Mol. Biol. 234 (1993) 938–945.
[2] E.E. Smith, B.M. Austen, K.M. Blumenthal, J.F. Nyc, Glutamate Dehydrogenases, Academic Press, New York, 1975.
[3] C. Werner, M.T. Stubbs, R.L. Krauth-Siegel, G. Klebe, The crystal structure of Plasmodium falciparum glutamate dehydrogenase, a putative target for novel antimalarial drugs, J. Mol. Biol. 349 (2005) 597–607.
[4] P.E. Peterson, T.J. Smith, The structure of bovine glutamate dehydrogenase provides insights into the mechanism of allostery, Structure 7 (1999) 769–782.
[5] S. Banerjee, T. Schmidt, J. Fang, C.A. Stanley, T.J. Smith, Structural studies on ADP activation of mammalian glutamate dehydrogenase and the evolution of regulation, Biochemistry 42 (2003) 3446–3456.

[6] K.L. Britton, P.J. Baker, D.W. Rice, T.J. Stillman, Structural relationship between the hexameric and tetrameric family of glutamate-dehydrogenases, Eur. J. Biochem. 209 (1992) 851–859.
[7] T.J. Stillman, P.J. Baker, K.L. Britton, D.W. Rice, H.F. Rodgers, Effect of additives on the crystallization of glutamate-dehydrogenase from Clostridium symbiosum – evidence for a ligand-induced conformational change, J. Mol. Biol. 224 (1992) 1181–1184.
[8] M.A. Sharkey, T.F. Oliveira, P.C. Engel, A.R. Khan, Structure of NADP(+)-dependent glutamate dehydrogenase from Escherichia coli–reflections on the basis of coenzyme specificity in the family of glutamate dehydrogenases, FEBS J. 280 (2013) 4681–4692.
[9] Z. Otwinowski, W. Minor, Processing of X-ray diffraction data collected in oscillation mode, Macromol. Crystallogr. Pt A 276 (1997) 307–326.
[10] B.W. Matthews, Solvent content of protein crystals, J. Mol. Biol. 33 (1968) 491–497.
[11] A. Vagin, A. Teplyakov, Molecular replacement with MOLREP, Acta Crystallogr. D. Biol. Crystallogr. 66 (2010) 22–25.
[12] P. Emsley, K. Cowtan, Coot: model-building tools for molecular graphics, Acta Crystallogr. D. Biol. Crystallogr. 60 (2004) 2126–2132.
[13] G.N. Murshudov, A.A. Vagin, E.J. Dodson, Refinement of macromolecular structures by the maximum-likelihood method, Acta Crystallogr. D. Biol. Crystallogr. 53 (1997) 240–255.
[14] A.T. Brunger, P.D. Adams, G.M. Clore, W.L. DeLano, P. Gros, R.W. Grosse-Kunstleve, J.S. Jiang, J. Kuszewski, M. Nilges, N.S. Pannu, R.J. Read, L.M. Rice, T. Simonson, G.L. Warren, Crystallography & NMR system: a new software suite for macromolecular structure determination, Acta Crystallogr. D. Biol. Crystallogr. 54 (1998) 905–921.
[15] M.G. Rossmann, D. Moras, K.W. Olsen, Chemical and biological evolution of nucleotide-binding protein, Nature 250 (1974) 194–199.
[16] C.A. Bottoms, P.E. Smith, J.J. Tanner, A structurally conserved water molecule in Rossmann dinucleotide-binding domains, Protein Sci. 11 (2002) 2125–2137.